Far-Field Radiation Properties of Impedance-Loaded Loop Antennas from RF to Optical Frequencies

Jogender Nagar[1*], Arnold F. McKinley[2], and Douglas H. Werner[1]
[1] School of Electrical Engineering and Computer Science, Penn State University, University Park, PA, USA
jun163@psu.edu*, dhw@psu.edu
[2] Department of Electronic and Electrical Engineering, University College London, London, UK, WC1E 7JE
arni.mckinley@ucl.ac.uk

***Abstract*—Impedance loading of antennas has been of interest for more than half a century due to its ability to fundamentally change an antenna's operating characteristics. Variable reactive loading can be employed for configurability of the frequency response, polarization and far-field properties of an antenna. Closed-form expressions for the current and input impedance of a thin-wire loop antenna with loads in the periphery were derived in the RF and optical regimes in 1965 and 2017, respectively. Meanwhile, closed-form far-field radiation properties of circular loop antennas in the RF and optical regimes were derived in 1996 and 2017. This paper extends this theory to provide closed-form analytical expressions for the far-field radiation properties of impedance-loaded loop antennas valid from the RF to the optical regimes. The expressions are validated by comparison with commercial simulation tools. In addition, a beam steering example is presented as a potential application of the theory.**

***Index Terms*—antennas, nano-antennas, adaptive and reconfigurable antennas, metamaterials.**

I. Introduction

As one of the fundamental and enabling components of wireless communications, antennas in the RF and optical regimes have a wide variety of applications, including biological sensing, solar energy harvesting and radar systems [1-2]. By loading an antenna with a resistive or reactive load, the fundamental operating characteristics such as the frequency response, polarization, radiation patterns and scattering properties can be dramatically altered [3]. Furthermore, tunable reactive loads are one of the most popular methods of achieving reconfigurable antennas, allowing the antenna to adapt based on system requirements or the environment [4]. Closed-form analytical expressions for the properties of impedance-loaded antennas enable rapid simulation and optimization, along with insight into the underlying physics governing the behavior of structures. In particular, loop antennas are one of the most fundamental and popular antennas due to their simplicity and wide range of practical applications [5].

Closed-form expressions for the current and input impedance of thin-wire perfectly conducting (PEC) loops were derived by Storer [6] and Wu [7]. Iizuka [8] extended the theory to include loads around the periphery of the antenna. Exact expressions for the near- and far-fields of circular (non-loaded) loops were derived by Werner [9]. The analytical theory for the current and input impedance of closed and impedance-loaded loops were later extended by McKinley *et al.* [10-11] to the optical regime by including the surface impedance effects of imperfect conductors. Finally, Lu *et al.* [12] extended the expressions for the far-field radiation properties of circular loops to the optical regime. This paper builds on these works by deriving closed-form expressions for the far-field radiation properties of impedance-loaded loops valid from the RF to optical regimes.

II. Theoretical Formulation

Fig. 1 shows the geometry of a circular loop with loop radius b and wire radius a which satisfies the thin-wire ($a^2 \ll b^2$) assumption. In this paper, the so-called "thickness measure" $\Omega = 2\ln(2\pi b/a)$ will be used to characterize the wire thickness. Loop antennas with $\Omega \geq 10$ satisfy the thin-wire assumption [11], where an infinitesimal voltage source with voltage V_0 is placed at $\varphi = 0$.

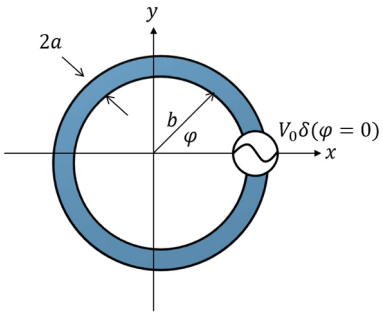

Fig. 1. Geometry of the thin-wire circular loop with loop radius b and wire radius a. A voltage source with constant voltage V_0 is placed at φ = 0.

The current can be expressed as a Fourier series [6-7]:

$$I(\varphi) = \sum_{m=-\infty}^{\infty} I_m e^{jm\varphi} = V_0 \left[\sum_{m=-\infty}^{\infty} Y'_m \, e^{jm\varphi} \right] \tag{1}$$

where the input admittances for each mode are given by:

$$\begin{aligned} Y'_0 &= [j\pi\eta_0 a_0 + (b/a)Z_s]^{-1} \\ Y'_m &= [j\pi\eta_0 (a_m/2) + (b/a)(Z_s/2)]^{-1} \end{aligned} \tag{2}$$

and where η_0 is the impedance of free space. The primed notation used here is to differentiate these modal admittances from those of Storer and Wu. Expressions for the coefficients a_m and the surface impedance Z_s are given explicitly in [10]. Following the notation of [11], the derivation for impedance-loaded loops starts by placing voltage sources $V_q\delta(\varphi)$ evenly spaced around the loop separated by an angle $\Delta\varphi = 2\pi/M$ where M is the number of impedances as shown in Fig. 2.

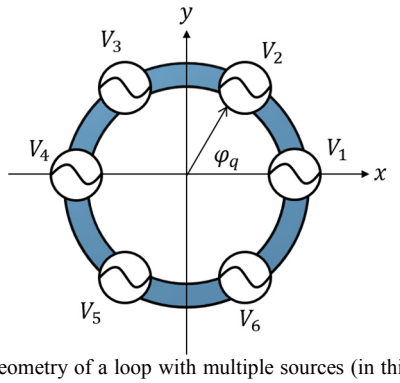

Fig. 2. Geometry of a loop with multiple sources (in this case, $M = 6$). Each voltage source V_q is placed at $\varphi = \varphi_q$.

The total current is a superposition of the currents due to each voltage source:

$$\begin{aligned} I(\varphi) &= \sum_{q=1}^{M}\left[\sum_{m=-\infty}^{\infty} Y'_m\, e^{jm\left(\varphi-\frac{2\pi(q-1)}{M}\right)}\right]V_q \\ &= \sum_{q=1}^{M} Y(\varphi,q)V_q \end{aligned} \tag{3}$$

The admittance at a source p is given by

$$Y(\varphi_p,q) = \sum_{m=-\infty}^{\infty} Y'_m\, e^{jm\left(\frac{2\pi(p-q)}{M}\right)} \tag{4}$$

These equations can concisely be written using matrix notation and the Einstein summation rule, where repeated indices are summed over. In addition, a horizontal vector will be denoted with an upper index, a vertical vector with a lower index and a matrix will contain both indices. For example, the term Y_p^q is a square M by M matrix of admittances as given in (4) and V_q is a vertical vector of voltages. Using this notation, (3) can be expressed as:

$$I(\varphi) = Y^q(\varphi)V_q \tag{5}$$

To include impedances in the analytical theory, series impedances are added to the voltage sources:

$$V_q \to V_q - Z_q^k I_k \tag{6}$$

where I_k is the current at φ_k and Z_q^k is a square M by M matrix in which the diagonal terms are the impedances and the off-diagonal terms are zero. Defining I_p^k as the identity matrix and

$$f_p^k \equiv I_p^k + Y_p^q Z_q^k \tag{7}$$

the current at any angle on the loop is given by [11]:

$$I'(\varphi) = Y^j(\varphi)V_j - Y^q(\varphi)Z_q^k[f^{-1}]_k^p Y_p^j V_j \tag{8}$$

where the primed notation indicates an impedance-loaded loop. Since this current is periodic (though not necessarily symmetric), it can be expressed as a Fourier series similar to (1):

$$I'(\varphi) = \sum_{m=-\infty}^{\infty} I_m e^{jm\varphi} \tag{9}$$

The current coefficients can be derived explicitly as:

$$\begin{aligned} I_m &= \tilde{Y}_m^l V_l - \tilde{Y}_m^q \tilde{V}_q \\ \tilde{Y}_m^l &= \sum_{l=1}^{M} Y'_m e^{-\frac{j2\pi n(l-1)}{M}} \\ \tilde{V}_q &= Z_q^k[f^{-1}]_k^p Y_p^l V_l \end{aligned} \tag{10}$$

Given the coefficients I_m in the Fourier expansion, the far-zone electric field can be expressed in spherical coordinates (θ,ϕ) for *the case of a symmetric current* where $w = k_b \sin\theta$ as [9]:

$$\begin{aligned} E_\theta &= -\frac{\eta_0 e^{-jk_0 r}\cot\theta}{2r}\sum_{m=1}^{\infty} mj^m I_m \sin(m\varphi) J_m(w) \\ E_\varphi &= -\frac{\eta_0 e^{-jk_0 r}k_b}{2r}\sum_{m=0}^{\infty} j^m I_m \cos(m\varphi) J'_m(w) \end{aligned} \tag{11}$$

in which J_m is a Bessel function of the first kind and J'_m is the derivative w.r.t. to the argument. When the loop is loaded with an impedance the current may no longer be symmetric and the far-zone fields become:

$$\begin{aligned} E'_\theta &= -j\frac{\eta_0 e^{-jk_0 r}\cot\theta}{2r}\sum_{m=1}^{\infty} mj^m\{I_m e^{jm\varphi} - I_{-m}e^{-jm\varphi}\}J_m(\mathrm{w}) \\ E'_\varphi &= -\frac{\eta_0 e^{-jk_0 r}k_b}{2r}\sum_{m=0}^{\infty} \epsilon_m j^m\{I_m e^{jm\varphi} - I_{-m}e^{-jm\varphi}\}J'_m(w) \\ \epsilon_m &= \begin{cases} 1/2 & m = 0 \\ 1 & m \neq 0 \end{cases} \end{aligned} \tag{12}$$

The radiated power can be derived by integrating the fields given in (12). The simplified expression can be written as:

$$P_r'(k_b) = \frac{\eta_0 \pi k_b^2}{2} |V_0|^2 T'(k_b) \tag{13}$$

$$T'(k_b) = \sum_{m=0}^{\infty} \epsilon_m \{|Y_m'|^2 + |Y_{-m}'|^2\} \left[\frac{1}{2} Q_{m-1\,m-1}^{(1)}(k_b) + \frac{1}{2} Q_{m+1\,m+1}^{(1)}(k_b) - \frac{m^2}{k_b^2} Q_{mm}^{(1)}(k_b)\right] \tag{14}$$

where $Q_{mn}^{(p)}(x)$ are the Q-type integrals defined in [13]. The radiation intensity at (θ, ϕ) is given in terms of normalized far-zone electric fields $E_\theta^0 = re^{jk_0 r} E_\theta$, $E_\varphi^0 = re^{jk_0 r} E_\varphi$, as:

$$U'(\theta, \varphi) = \frac{1}{2\eta_0} \left[\left|E_\theta^{0\prime}\right|^2 + \left|E_\varphi^{0\prime}\right|^2\right] \tag{15}$$

where, from (12):

$$\left|E_\theta^{0\prime}\right|^2 = \frac{|V_0|^2 \eta_0^2 \cot^2\theta}{4} \sum_{m=-\infty}^{\infty} \sum_{n=-\infty}^{\infty} \begin{bmatrix} mn(-1)^n j^{m+n} Y_m' Y_n'^* e^{j(m-n)\varphi} \cdot \\ J_m(k_b \sin\theta) J_n(k_b \sin\theta) \end{bmatrix}$$

$$\left|E_\varphi^{0\prime}\right|^2 = \frac{|V_0|^2 \eta_0^2 k_b^2}{4} \sum_{m=-\infty}^{\infty} \sum_{n=-\infty}^{\infty} \left[\begin{matrix} (-1)^n j^{m+n} Y_m' Y_n'^* e^{j(m-n)\varphi} \\ J_m'(k_b \sin\theta) J_n'(k_b \sin\theta) \end{matrix}\right] \tag{16}$$

The directivity is given by:

$$D'(\theta, \varphi) = \frac{4\pi U(\theta, \varphi)}{P_r'(k_b)} \tag{17}$$

The loss resistance is expressed as:

$$R_{loss}' = \frac{b}{a} \frac{\mathrm{Re}(Z_s)}{|I_{in}|^2} \frac{1}{2\pi} \int_0^{2\pi} |I'(\varphi)|^2 d\varphi \tag{18}$$

Substituting (9) into (18) yields:

$$R_{loss}' = \mathrm{Re}(Z_s) \frac{b}{a} |Z_{in}'|^2 \sum_{m=0}^{\infty} \epsilon_m \{|Y_m'|^2 + |Y_{-m}'|^2\} \tag{19}$$

The input radiation resistance is given by:

$$R_{rad,in}' = \frac{2P_r'(k_b)}{|I_{in}'|^2} = \frac{2P_r'(k_b)|Z_{in}'|^2}{|V_0|^2} \tag{20}$$

Substituting (13) into (20) results in:

$$R_{rad,in}' = k_b^2 \pi \eta_0 \left|Z_{in}^{'}\right|^2 T(k_b) \tag{21}$$

Finally, the gain may be obtained from:

$$G'(\theta, \varphi) = e' D'(\theta, \varphi) = \frac{R_{rad,in}}{R_{rad,in} + R_{loss}} D'(\theta, \varphi) \tag{22}$$

III. Validation

In order to validate the derived expressions, the closed-form solutions of (9)-(22) were implemented in MATLAB [14] and compared to the commercial full-wave method of moments solver FEKO [15]. The unit-less parameters r, l_ϵ, and l_μ for the resistance, capacitance and inductance will be used to describe a general load:

$$Z_L \equiv \eta_0 \left[r + j\left(k_b l_\mu - \frac{1}{k_b l_\epsilon}\right)\right] \tag{23}$$

As a validation test case, a resistive ($r = 4$), inductive ($l_\mu = 0.5$) and capacitive load ($l_\epsilon = 0.5$) will be placed at $\varphi = 180$ for a PEC loop with $\Omega = 12$ at $k_b = 1.06$ and the results from the analytical theory and FEKO will be compared. Fig. 3 shows a comparison of the real and imaginary current versus φ for a closed (unloaded) loop and a loop with the three different types of loads. As can be seen, there is excellent agreement in all cases.

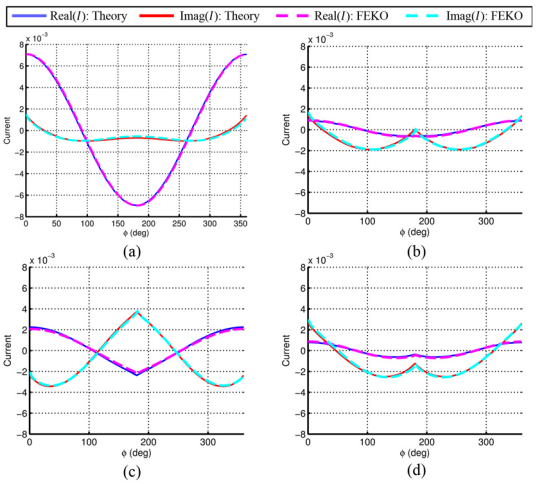

Fig. 3. Comparison between the analytical theory and FEKO for the real and imaginary components of the current for the (a) unloaded loop and the impedance-loaded loop with (b) $r = 4$, (c) $l_\mu = 0.5$ and (d) $l_\epsilon = 0.5$.

Fig. 4 shows a comparison of the magnitude of the far-zone electric field for all four cases; again, there is very good agreement between the theory and the numerical simulation.

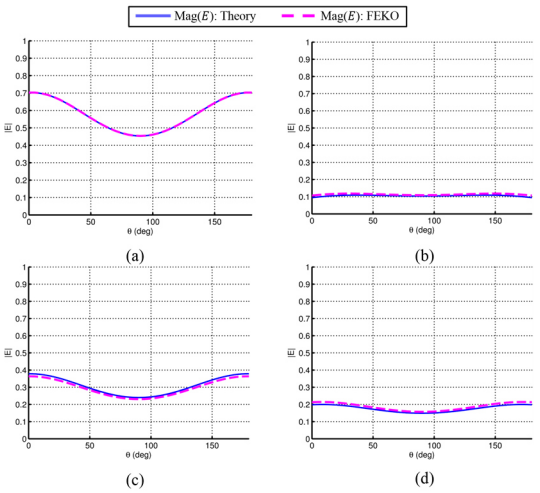

Fig. 4. Comparison between the analytical theory and FEKO for the magnitude of the far-zone electric field for the (a) unloaded loop and the impedance-loaded loop with (b) $r = 4$, (c) $l_\mu = 0.5$ and (d) $l_\epsilon = 0.5$.

IV. Beam Steering Example

Next, an example application of an impedance-loaded PEC loop will be discussed. At the first high-Q resonance $k_b = 0.3437$ a capacitive load with $l_\epsilon = 1$ can be placed around the periphery of the loop to steer the beam in the plane of the loop. Fig. 5 shows the directivity in dB when φ_q is varied from 0 to π with increments of $\pi/6$. Fig. 6 shows the 3D radiation patterns, where the beam steering effect can clearly be seen.

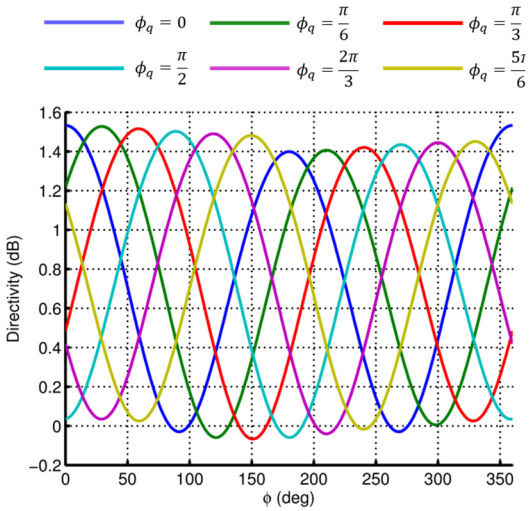

Fig. 5. Directivity in dB when a capacitive load with $l_\epsilon = 1$ is placed at $\varphi_q = \left[0, \frac{\pi}{6}, \frac{\pi}{3}, \frac{\pi}{2}, \frac{2\pi}{3}, \frac{5\pi}{6}\right]$.

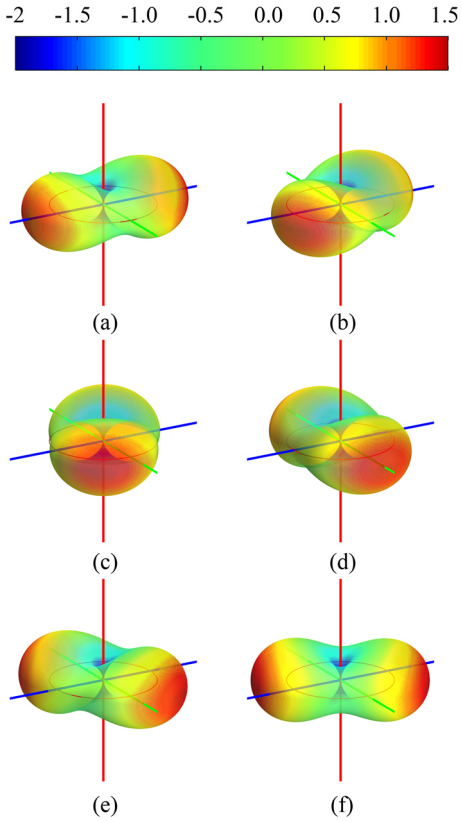

Fig. 6. 3D directivity patterns in dB when a capacitive load with $l_\epsilon = 1$ is placed at (a) $\phi_q = 0$, (b) $\phi_q = \pi/6$, (c) $\phi_q = \pi/3$, (d) $\phi_q = \pi/2$, (e) $\phi_q = 2\pi/3$ and (f) $\phi_q = 5\pi/6$.

V. Conclusion

This paper presented closed-form analytical expressions for the far-field radiation properties of impedance-loaded loops valid from the RF to optical regimes. The analytical theory was validated by comparison with the commercial full-wave method of moments solver FEKO. A potential application of the theory was presented through an example in which the far-field beam could be steered in the plane of the loop through the strategic placement of a capacitive load on the periphery of the loop. Further work includes validation of the proposed theory for a gold nanoloop, along with more examples demonstrating potential applications of the theoretical analysis.

Acknowledgment

Partial support for this work was provided by the Center for Nanoscale Science, an NSF Materials Research Science and Engineering Center, under the award DMR-1420620.

References

[1] C. A. Balanis, *Antenna Theory*. New York: Wiley, 1997.

[2] L. Novotny, and B. Hecht, *Principles of Nano-Optics*. Cambridge, UK: Cambridge University Press, 2012.

[3] Y. Chen and C.-F. Wang, *Characteristic Modes: Theory and Applications in Antenna Engineering*. New Jersey: John Wiley & Sons, 2015.

[4] J. T. Bernhard, "Reconfigurable antennas," *Synthesis Lectures on Antennas*, vol. 2, no. 1, pp. 1-66, 2007.

[5] G. S. Smith, "Loop antennas," in *Antenna Engineering Handbook,* R. Johnson, Ed. New York: McGraw-Hill, 1993.

[6] J. E. Storer, "Impedance of thin-wire loop antennas," *Trans. Amer. Inst. Elect. Eng*., vol. 75, pp. 606–619, Nov. 1956.

[7] T. T. Wu, "Theory of the thin circular loop antenna," *J. Math. Phys*., vol. 3, no. 6, pp. 1301–1304, 1962.

[8] K. Iizuka, "The circular loop antenna multiloaded with positive and negative resistors," *IEEE Trans. Antennas Propag*., vol. 13, no. 1, pp. 7–20, Jan. 1965.

[9] D. H. Werner, "An exact integration procedure for vector potentials of thin circular loop antennas," *IEEE Trans. Ant. and Prop.,* vol. 44, pp. 157-165, 1996.

[10] A. F. McKinley, T. P. White, and K. R. Catchpole, "Theory of the circular closed loop antenna in the terahertz, infrared, and optical regions," *J. Appl. Phys*., vol. 114, no. 4, p. 044317, 2013.

[11] A. F. McKinley, "Theory of impedance loaded loop antennas and nanorings from RF to optical wavelengths," *IEEE Trans. Ant. and Prop.,* vol. 65, no. 5, pp. 2276-2281, 2017.

[12] B. Q. Lu, J. Nagar, T. Yue, M. F. Pantoja and D. H. Werner, "Closed-form expressions for the radiation properties of nanoloops in the terahertz, infrared and optical regimes," *IEEE Trans. Ant. and Prop.,* vol. 65, no. 1, pp. 121-133, 2017.

[13] S. V. Savov, "An efficient solution of a class of integrals arising in antenna theory," *IEEE Ant. and Prop. Mag*., vol. 44, no. 5, pp. 98-101, Oct. 2002.

[14] MATLAB R2014A, Mathworks – Natick, MA, USA, https://www.mathworks.com/

[15] FEKO Suite 7.0, EM Software & Systems - S.A., Stellenbosch, South Africa, http://www.feko.info